Structure, Composition, and Peptide Binding Properties of Detergent Soluble Bilayers and Detergent Resistant Rafts

M. Gandhavadi,* D. Allende,* A. Vidal,* S. A. Simon,† and T. J. McIntosh*
*Department of Cell Biology and †Department of Neurobiology, Duke University Medical Center, Durham, North Carolina 27710 USA

ABSTRACT Lipid bilayers composed of unsaturated phosphatidylcholine (PC), sphingomyelin (SM), and cholesterol are thought to contain microdomains that have similar detergent insolubility characteristics as rafts isolated from cell plasma membranes. We chemically characterized the fractions corresponding to detergent soluble membranes (DSMs) and detergent resistant membranes (DRMs) from 1:1:1 PC:SM:cholesterol, compared the binding properties of selected peptides to bilayers with the compositions of DSMs and DRMs, used differential scanning calorimetry to identify phase transitions, and determined the structure of DRMs with x-ray diffraction. Compared with the equimolar starting material, DRMs were enriched in both SM and cholesterol. Both transmembrane and interfacial peptides bound to a greater extent to DSM bilayers than to DRM bilayers, likely because of differences in the mechanical properties of the two bilayers. Thermograms from 1:1:1 PC:SM:cholesterol from 3 to 70°C showed no evidence for a liquid-ordered to liquid-disordered phase transition. Over a wide range of osmotic stresses, each x-ray pattern from equimolar PC:SM:cholesterol or DRMs contained a broad wide-angle band at 4.5 Å, indicating that the bilayers were in a liquid-crystalline phase, and several sharp low-angle reflections that indexed as orders of a single lamellar repeat period. Electron density profiles showed that the total bilayer thickness was 57 Å for DRMs, which was ~5 Å greater than that of 1:1:1 PC:SM:cholesterol and 10 Å greater than the thickness of bilayers with the composition of DSMs. These x-ray data provide accurate values for the widths of raft and nonraft bilayers that should be important in understanding mechanisms of protein sorting by rafts.

INTRODUCTION

Over the past several years evidence has accumulated implicating the presence of dynamic lipid/protein microdomains or "rafts" in cell plasma membranes (Simons and Ikonen, 1997, 2000; Brown and London, 1998, 2000; Harder et al., 1998) and the Golgi apparatus (Gkantiragas et al., 2001). Such rafts, which have been characterized by their insolubility in detergents such as Triton X-100 (Hanada et al., 1995; Brown and London, 2000; Simons and Ikonen, 2000), are enriched in cholesterol and sphingolipids (MacDonald, 1980; Hanada et al., 1995; Fridriksson et al., 1999; Brown and London, 2000). Whereas some membrane proteins are excluded from rafts, others are associated with them (Rodgers et al., 1994; Arreaza and Brown, 1995; Field et al., 1997; Brown and London, 1998; Melkonian et al., 1999; Baird et al., 1999; Moffett et al., 2000; Prinetti et al., 2000; Galbiati et al., 2001). Primarily due to their ability to sequester specific classes of lipids and proteins, rafts are postulated to perform roles in a number of important cellular processes, such as signal transduction (Field et al., 1997; Brown and London, 1998; Solomon et al., 1998; Baird et al., 1999; Kawabuchi et al., 2000; Moffett et al., 2000), membrane fusion (Chamberlain et al., 2001; Lang et al., 2001), membrane budding (Huttner and Zimmerberg, 2001), and protein trafficking (Bretscher and Munro, 1993; Simons and Ikonen, 1997, 2001; Lafont et al., 1999; Ikonen, 2001).

Two key features of rafts that may be important in sorting membrane proteins involve potential structural and mechanical differences between raft bilayers and other bilayers. First, due to their high concentrations of cholesterol and sphingolipids with long, saturated hydrocarbon chains, rafts may have thicker bilayers than the surrounding lipid matrix containing unsaturated phospholipids (Bretscher and Munro, 1993). This structural feature is postulated to be important in protein trafficking through the Golgi apparatus, as proteins with relatively long transmembrane hydrophobic regions would be expected to localize in the thick raft bilayers, whereas shorter transmembrane proteins should localize in the thinner nondomain regions (Bretscher and Munro, 1993; Munro, 1995). Consistent with this concept, experiments using lipid bilayers and peptides have shown that mismatch between the peptide transmembrane α-helix length and bilayer thickness can modify peptide conformation, orientation, and extent of bilayer incorporation (Webb et al., 1998; Killian, 1998; Ren et al., 1999; dePlanque et al., 2001). However, the thickness of unsupported raft membrane bilayers has not been accurately measured, and several recent depictions of rafts (Brown and London, 2000; Simons and Ikonen, 2000; Galbiati et al., 2001) do not show any difference in thickness between rafts and the surrounding membrane. Second, compared with other bilayers, sphingomyelin:cholesterol bilayers have larger compressibility moduli and hence cohesive energies (Needham and Nunn, 1990; McIntosh et al., 1992a), and therefore more energy should be required to separate adjacent lipid molecules in the plane of the bilayer for rafts than for typical

Submitted October 24, 2001, and accepted for publication November 1, 2001.

Address reprint requests to Thomas J. McIntosh, Department of Cell Biology, Duke University Medical Center, 443 Sands Building, Durham, NC 27710. Tel.: 919-684-8950; Fax: 919-681-9929; E-mail: t.mcintosh@cellbio.duke.edu.

0006-3495/02/03/1469/14 $2.00

lipid bilayers. Therefore, we hypothesize that the partition coefficient should be smaller for the binding of amphipathic peptides or hydrophobic regions of proteins to rafts than to nonraft membranes.

Both the lateral size and mechanism of formation of membrane rafts are controversial (Edidin, 1998; Kenworthy and Edidin, 1998; Kenworthy et al., 2000). In cells, estimates of raft size range from hundreds of nanometers (Sheets et al., 1997; Schutz et al., 2000) to a few nanometers (Scheiffele et al., 1997). Several factors may be involved in the formation and maintenance of membrane domains, including lipid-lipid interactions (Simons and van Meer, 1988; Bretscher and Munro, 1993; Ahmed et al., 1997), lipid-cytoskeleton interactions (Gheber and Edidin, 1999; Oliferenko et al., 1999; Babiychuk and Draeger, 2000; Foger et al., 2001; Tang and Edidin, 2001), and vesicle trafficking to the plasma membrane (Gheber and Edidin, 1999; Tang and Edidin, 2001).

Domain formation involving lipid-lipid interactions is postulated to be critical for trafficking of membrane proteins through the Golgi apparatus (Simons and van Meer, 1988; Bretscher and Munro, 1993), and recent work has indicated that, even in the absence of proteins, lipid domains can form in bilayers containing specific lipid compositions. For example, Ahmed et al. (1997), Xu and London (2000), and Wang et al. (2000) found indications of phase separation in multilamellar vesicles containing three components: 1) lipids that form gel phases at physiological temperatures, such as dipalmitoylphosphatidylcholine (DPPC) or sphingomyelin (SM), 2) phospholipids that form liquid-crystalline bilayers at physiological temperatures, such as dioleoylphosphatidylcholine (DOPC), and 3) cholesterol. Because, for cholesterol concentrations greater than 25 mol%, DPPC:cholesterol is in a "liquid-ordered" phase, a liquid-crystalline phase with more conformationally ordered hydrocarbon chains than a "liquid-disordered" phase (Ipsen et al., 1987), Ahmed et al. (1997) argued that the detergent-resistant membrane phase (DRM) represents a liquid-ordered phase (rich in DPPC:cholesterol or SM:cholesterol) related to DRMs found in cell membranes, whereas the detergent-soluble membrane phase (DSM) represents a liquid-disordered phase (rich in DOPC). Recently micron-sized domains have been observed by fluorescence light microscopy or atomic force microscopy (AFM) for DOPC:SM:cholesterol in a variety of bilayer preparations, including supported bilayers (Dietrich et al., 2001; Rinia et al., 2001), giant unilamellar vesicles (GUVs) (Dietrich et al., 2001), and planar lipid bilayers (Samsonov et al., 2001). The presence and size of the domains depended reversibly on temperature. In GUVs large domains were visible at 25°C but not at 30°C (Dietrich et al., 2001), and in planar bilayers the percentage of raft area was reduced when the temperature was raised above the phase transition of SM (48°C for egg SM) (Samsonov et al., 2001).

In this paper we further characterize lipid vesicles containing a DOPC:SM:cholesterol composition studied by Ahmed et al. (1997), Rinia et al. (2001), and Dietrich et al. (2001). We isolate and chemically characterize detergent resistant membranes (DRMs, analogs of membrane rafts) and detergent soluble membranes (DSMs) from these vesicles and use x-ray diffraction to determine the hydrocarbon chain packing and relative bilayer thicknesses of the total lipid mixture, DRMs, and DSMs. Differential scanning calorimetry (DSC) is used to search for a phase transition in the temperature range where light microscopy demonstrated a phase change from two domains (rafts and matrix bilayer) to a single matrix domain (Dietrich et al., 2001; Samsonov et al., 2001). To determine the interactive properties of the DRMs and DSMs, we measure and compare: 1) their total interbilayer pressures and 2) their binding to both transmembrane and interfacial peptides. The binding experiments provide information as to whether bilayers with the compositions of DRMs and DSMs can distinguish among different peptides.

MATERIALS AND METHODS

Materials

DOPC, DPPC, and bovine brain SM were purchased from Avanti Polar Lipids (Alabaster, AL). Cholesterol, cholesterol infinity reagent, benzidine, polyvinylpyrrolidone (PVP), melittin, and Triton X-100 were purchased from Sigma Chemical Company (St. Louis, MO), and SM-2 adsorbent BioBeads were purchased from BioRad (Hercules, CA). The BioBeads were successively washed in water, 1 M acetic acid, methanol, and water, whereas all of the other compounds were used without further purification.

The peptides BR-C (the third or C transmembrane α-helix of bacteriorhodopsin, amino acid sequence GGEQNPIYWARYADWLFTTPLLLLDLALLVDADEGT) and MPR (the presequence of the mitochondrial protein rhodanese, amino acid sequence MVHQVLYRALVSTKWLAESIRSG) were synthesized by the Micro Protein Chemistry Facility at the University of North Carolina (Chapel Hill, NC) using FMOC chemistry in a Symphony (Rainin) peptide synthesizer. These peptides were purified by HPLC and analyzed by time-of-flight MALDI III (Shimadzu/Kratos) mass spectrometry.

Preparation of vesicles for x-ray diffraction and peptide binding experiments

Multilamellar lipid vesicles (MLVs) were made by the following procedure. The appropriate lipids were codissolved in chloroform or chloroform:methanol (3:1 v/v). The solvent was removed by rotary evaporation, and the dry lipid was subsequently hydrated with PVP solutions (0–40% PVP) made in either 25 mM KCl, 5 mM Hepes buffer (pH 7.4), or water. No difference was observed in x-ray experiments or chemical analyses for samples prepared with this buffer or with water.

For peptide binding experiments, small unilamellar vesicles (SUVs) and large unilamellar vesicles (LUVs) were prepared from MLVs by the following procedures. To make SUVs, MLVs in 25 mM KCl, 5 mM Hepes buffer (pH 7.4) were sonicated for 10 cycles of 4-min duration (2-min sonication and 2-min stand by) at 40 W with a 19-mm flat tip probe sonicator (Misonix, Farmingdale, NY). To sediment any remaining MLVs and titanium particles detached from the probe, the dispersions were centrifuged at 100,000 $\times$ g for 10 min. LUVs were formed from MLVs

using the extrusion method (Hope et al., 1985). MLVs, at concentrations of 5 to 15 mg/ml, were frozen and thawed 3 times and extruded 20 times through a 0.1-μm polycarbonate filter with a LiposoFast lipid extruder (Avestin, Ottawa, Canada). For binding experiments using the ultracentrifugation method described below, LUVs were loaded with sucrose by initially forming the MLVs in 48 mM sucrose solution and then washing the extruded LUVs with isoosmotic buffer (25 mM KCl) (Buser and McLaughlin, 1998). After either sonication or extrusion, phospholipid concentrations were measured by phosphate analysis (Chen et al., 1956).

Detergent extraction and chemical analysis of DRMs and DSMs

Detergent extraction procedures were similar to those of Ahmed et al. (1997). MLVs of 1:1:1 DOPC:SM:cholesterol in either water or buffer (total lipid concentration 3–4 mg/ml) were treated with Triton X-100 for 30 min at 4°C and then centrifuged 30 min at 4°C with an Eppendorf bench centrifuge. One percent Triton X-100 was used in most experiments, although 0.1% and 4% Triton X-100 were used in some TLC and x-ray experiments as described. The supernatant was removed and the pellet was resuspended in an equal volume of buffer or water and probe sonicated. The phospholipid content of the supernatant (containing DSMs) and resuspended pellet (DRMs) were determined by phosphate assay (Chen et al., 1956), and the cholesterol content was determined using the Sigma infinity (cholesterol oxidase) assay.

To reduce the Triton X-100 concentration before thin layer chromatography (TLC) or x-ray diffraction analysis, the DSMs and DRMs were washed three times for 90 min with SM-2 BioBeads (100 mg/ml). TLC was performed using chloroform:methanol:ammonium hydroxide 65:25:4 (v/v) as the solvent. For most of these experiments iodine vapor was used to detect the lipid spots, and lanes with DOPC and SM controls were used to identify the location of the DOPC and SM spots. In some experiments, benzidine reagent, which stains sphingolipids but not PCs (Kates, 1972), was used to verify the location of SM on the TLC plate. To estimate the DOPC to SM ratio in the DRMs and DSMs, the ratios of the densities of the respective spots in the iodine-treated TLC plates were compared with those of control iodine-treated TLC plates containing lanes with 9:1, 8:2, 7:3, 6:4, 5:5, 4:6, 3:7, 2:8, and 1:9 mol ratios of DOPC:SM. Relative densities of the DOPC and SM spots were determined by obtaining color scans with an AGFA T2500 Scanner (Agfa-Gervaert N. V., Mortsel, Belgium), converting these scans to grayscale TIFF format through Adobe Photoshop 5.0, and then using NIH Image Version 1.61 to measure the area under each peak.

X-ray diffraction

The structures of the lipid systems were obtained by x-ray diffraction analysis of both the unoriented MLV suspensions and oriented multilayers by techniques described in detail previously (McIntosh et al., 1987, 1989a, 1992a,b). In brief, unoriented MLVs in PVP solutions of various concentrations were pelleted, sealed in glass x-ray capillary tubes, and mounted in a temperature-controlled specimen chamber in a point collimation x-ray camera. For PVP solutions from 0 to 40% PVP the osmotic pressures (P) were in the range of 0 to 1×10^7 dyn/cm^2 (Parsegian et al., 1986; McIntosh and Simon, 1986). Oriented lipid multilayers were prepared by placing a drop of an aqueous suspension of MLVs, DRMs, or DSMs onto a curved glass substrate and drying it under a gentle stream of nitrogen. For osmotic pressures in the range 1×10^7 dyn/cm^2 to 1×10^9 dyn/cm^2 the lipid multilayers oriented on the glass substrate were mounted in a temperature-controlled constant humidity sample chamber on a line-focus (single mirror) x-ray camera (McIntosh et al., 1987, 1989a). Relative humidities from 98 to 66% were set by incubation with saturated salt solutions (McIntosh et al., 1987, 1989a, 1992a; Kulkarni et al., 1999). X-ray patterns were recorded at ambient temperature on Kodak DEF-5 x-ray film.

To obtain electron density profiles across the bilayer, a Fourier analysis of the x-ray diffraction patterns was performed. Integrated intensities were obtained for each diffraction order by measuring the area under each diffraction peak, and structure amplitudes were obtained by applying standard correction factors for either oriented or unoriented specimens (McIntosh and Simon, 1986; McIntosh et al., 1987). As described in detail previously (McIntosh and Simon, 1986; McIntosh et al., 1987, 1992a,b), phase angles were determined by using the osmotic stress experiments to trace out the continuous transform of the bilayer. For each bilayer system continuous transforms were calculated by use of the sampling theorem (Shannon, 1949) for one data set for each possible phase combination. The phase combination that gave the best match to the other structure factors was selected (McIntosh et al., 1984, 1987; McIntosh and Holloway, 1987). Electron density profiles across the bilayer were calculated from Fourier reconstructions using the x-ray structure factors

$$\rho(x) = (2/d)\Sigma\exp\{i\phi(h)\}F(h)\cos(2\pi xh/d) \qquad (1)$$

in which $F(h)$ is the x-ray structure amplitude, x is the distance from the center of the bilayer, d is the lamellar repeat period, $\phi(h)$ is the phase angle of order h (either 0 or 180° for these centrosymmetric systems), and the sum is over h.

Differential scanning calorimetry

Differential scanning calorimetry (DSC) was performed on MLVs using a VP-DSC microcalorimeter (MicroCal Inc., Northampton, MA). Before beginning a heating cycle the dispersion was incubated at 3°C for 30 min. Samples were cycled at least twice to insure that the thermograms were reproducible. The thermograms were obtained at heating rates of 15°C/h, and the data were analyzed using MicroCal software.

Peptide binding measurements

For peptide binding experiments, MPR and melittin were used at 5 and 10 μM concentrations, respectively, in 5 mM Hepes, 25 mM KCl, pH 7.4. At these concentrations MPR (Wieprecht et al., 2000) and melittin (Faucon et al., 1979; Quay and Condie, 1983) are monomeric. The binding of these peptides to SUVs or LUVs was measured with an ultrafiltration assay (Sophianopoulos et al., 1978) that separated lipid and lipid/peptide complexes from free peptide with Centricon-10 filters (Millipore Inc., Bedford, MA). Peptide was added to SUVs or LUVs and incubated for 30 min before a 1-h centrifugation at $6000 \times g$ through the filter (Voglino et al., 1998, 1999). The free peptide concentration in the eluate was determined by measuring tryptophan fluorescence at an emission wavelength of 340 nm (for MPR) or 356 nm (for melittin) in a Jobin Yvon SPEX fluorometer DM-3000 and comparing to fluorescence-concentration standards obtained for each peptide. The amount of peptide bound to the lipid was determined by subtracting the free peptide concentration from the total peptide concentration.

For BR-C a different hydration protocol was used because of the limited water solubility of the peptide (Hunt et al., 1997). Briefly, 0.5 mg/ml of lyophilized peptide was solubilized in 6 M urea, 200 mM NaCl, 10 mM Tris, pH 8.3, and then dialyzed twice against the same buffer without urea (Hunt et al., 1997). This was followed by three dialysis runs in 20 mM NaCl, 5 mM $NaPO_4$, pH 8.0. The total dialysis time was greater than 30 h, and the buffer was changed every 3 h. Because control experiments showed that the BR-C peptide adhered to the Centricon filters, an ultracentrifugation method (Buser and McLaughlin, 1998) was used to measure binding for this peptide. With this procedure, BR-C was incubated with sucrose-loaded LUVs and then titrated to pH 5.5 with HCl. Experiments by Hunt et al. (1997) show that at this pH the BR-C partitions so that it is in a transmembrane orientation in the bilayer. The samples were centrifuged for 1 h at 43,000 rpm in a Beckman ultracentrifuge TLA-100. The concentra-

TABLE 1 Chemical analysis of DRMs and DSMs isolated from 1:1:1 DOPC:SM:cholesterol

% Triton X-100	DRM/DSM phospholipid (mol ratio)	DRMs PL/cholesterol (mol ratio)	DRMs DOPC/SM (mol ratio)	DSMs PL/cholesterol (mol ratio)	DSMs DOPC/SM (mol ratio)
0.1%	9.9	2.0	0.76	—	>9.0
1.0%	1.6	1.5	0.32	4.1	>9.0
4.0%	1.3	—	0.19	—	>9.0

tion of peptide in the supernatant was measured by fluorescence at 340 nm as described above.

For the water-soluble peptides MPR and melittin, under conditions where the molar concentration of peptide in the bilayer is much smaller than the molar concentration of lipid, the mole fraction partition coefficient (K_p) can be written as

$$K_p = (P_{bil}W)/(P_{wat}L) \quad (2)$$

in which P_{bil} and P_{wat} are the bulk molar concentrations of peptide in the bilayer and water phases, respectively, and L and W are the molar concentrations of lipid and water, respectively (Ladokhin et al., 1997). It is assumed that at these low peptide concentrations the amphipathic peptides MPR and melittin partition only into the outer monolayer of the bilayer, so L was taken as the amount of total lipid in the outer monolayer (66% for SUVs). In the case of BR-C, the peptide aggregates in solution (Hunt et al., 1997) so partition coefficients could not be calculated. Therefore, for BR-C we present binding data only in terms of the percent peptide bound to the bilayer.

RESULTS

Chemical characterization of DRMs and DSMs

As shown in Table 1, the ratio of phospholipid in the DRMs to that in the DSMs decreased with increasing Triton X-100 concentration. That is, more phospholipid was solubilized with increasing concentration of detergent. In a similar manner in DRMs, the DOPC/SM ratio, as determined by TLC (Fig. 1), decreased with increasing Triton X-100 concentration, whereas the DOPC/SM ratio in DSMs was always large (>9). The phospholipid/cholesterol ratio, as measured by a combination of phosphorous and cholesterol oxidase assays, showed that for 1% Triton X-100 treatment the phospholipid/cholesterol ratio was significantly higher in DSMs (4.1 ± 1.2, mean ± SD, $n = 3$ experiments) than in DRMs (1.5 ± 0.2). Control experiments with 2:1 DOPC:cholesterol and 2:1 SM:cholesterol showed that the cholesterol assay provided accurate determinations for cholesterol contents (<10% error) for vesicles containing 1% Triton X-100 or less. However, because considerably larger errors (20–30%) were obtained in control experiments with 4% Triton X-100, the cholesterol oxidase assay was not used for the 4% Triton experiments. In addition, the cholesterol content in DSMs with 0.1% Triton X-100 treatment was below the sensitivity of the cholesterol oxidase assay (Table 1).

Taken together the data presented in Fig. 1 and Table 1 show that, compared with the starting equimolar DOPC:SM:cholesterol dispersion, the DRMs were highly enriched in both SM and cholesterol, whereas the DSMs were enriched in DOPC. Thus, the primary lipid solubilized by detergent treatment was DOPC, consistent with detergent extraction experiments with similar liposomal preparations (Schroeder et al., 1994).

X-ray diffraction

All x-ray diffraction patterns from 1:1:1 DOPC:SM:cholesterol at 20°C consisted of a single broad wide-angle band centered at 4.5 Å and several sharp low-angle reflections that indexed as the orders of a single lamellar repeat period. These patterns were consistent with multilayers of bilayers in a liquid-crystalline phase (Tardieu et al., 1973). As shown in Fig. 2, the low-angle region of a pattern recorded for 1:1:1 DOPC:SM:cholesterol MLVs in excess water (no applied osmotic pressure) consisted of several orders of a 67.6 Å repeat period. Notice that each of these reflections was quite sharp and that there was no indication of reflections corresponding to a second phase. In contrast, for 1:1 DOPC:SM in excess water, with no cholesterol present, the wide-angle patterns contained both a weak broad band at 4.5 Å (consistent with a liquid-crystalline phase) and a sharp reflection at 4.2 Å (consistent with a gel phase), and the low-angle pattern (Fig. 2) contained reflections with two

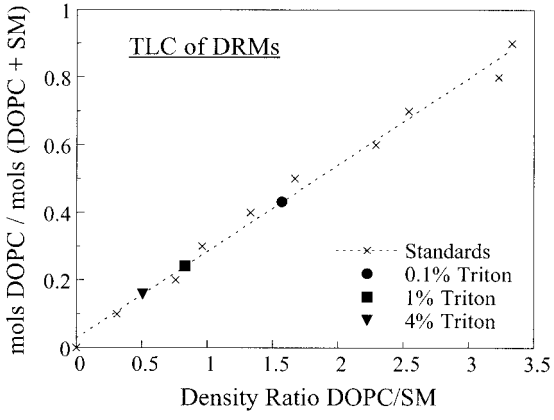

FIGURE 1 Results from thin layer chromatography of DRMs obtained with 0.1, 1.0, and 4% Triton X-100. The mole ratio of DOPC/(DOPC + SM) is plotted versus the density ratio of the DOPC and SM spots on TLC plates from DRMs. ×, Results from standards with mole ratios of DOPC/(DOPC + SM) varying from 0.0 to 0.9, and the dotted line is a least squares linear fit to the standard data ($R^2 = 0.989$).

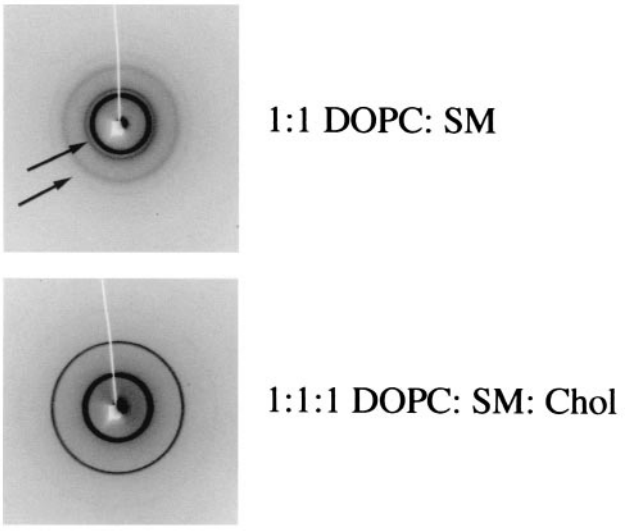

FIGURE 2 Low-angle x-ray diffraction patterns of 1:1 DOPC:SM (*top*) and 1:1:1 DOPC:SM:cholesterol (*bottom*) from a point-focus x-ray camera. In each pattern, the beam stop is at the center of the film and a series of circular reflections are present. In the case of 1:1:1 DOPC:SM:cholesterol three sharp, evenly spaced concentric rings are observed, indexing as the first three orders of a lamellar phase with repeat period of 67.6 Å. For 1:1 DOPC:SM four reflections are visible corresponding to the first two orders of two lamellar phases of repeat period of 76.6 Å and 63.3 Å. Arrows note the first two orders of the 63.3 Å lamellar phase.

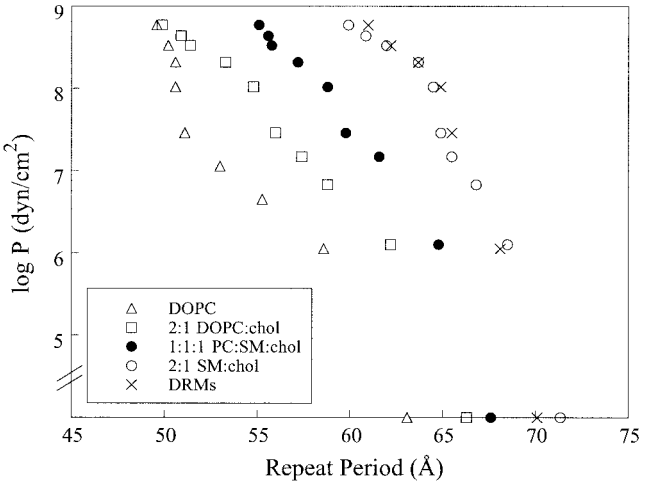

FIGURE 3 X-ray diffraction lamellar repeat periods obtained as a function of applied osmotic pressure (*P*) for bilayers composed of DOPC, 2:1 DOPC:cholesterol, 1:1:1 DOPC:SM:cholesterol, 2:1 SM:cholesterol, and DRMs isolated with 1% Triton X-100. Osmotic stresses were applied either by swelling multiwalled liposomes in PVP solutions (0 to 10^7 dyn/cm^2) or by incubating oriented multilayers in constant relative humidity atmospheres (10^7 to 10^9 dyn/cm^2). Data from MLVs in water with no applied pressure are shown on the *x* axis. For each sample, reflections were recorded that corresponded to orders of a single lamellar phase whose repeat period is indicated in this figure.

different lamellar repeat periods, 63.3 Å and 76.6 Å, that corresponded to the repeat periods observed for separate samples in excess water of DOPC or SM, respectively. Thus, in excess water 1:1 DOPC:SM bilayers phase separated to form liquid-crystalline and gel phases, whereas 1:1:1 DOPC:SM:cholesterol bilayers formed a single liquid-crystalline phase.

The presence of separate phases in x-ray patterns from DOPC:SM bilayers depended on both the lipid composition and the osmotic pressure (*P*). The application of large osmotic pressures tended to promote phase separation. For instance, for 7:3 DOPC:SM bilayers no phase separation was observed for samples in excess water, but patterns that indexed as two lamellar phases were observed at an osmotic pressure of 3×10^8 dyn/cm^2. Similar results have previously been found for bilayers of eggPC and the ganglioside GM1; no phase separation was observed at low osmotic pressures but two distinct lamellar phases were observed at osmotic pressures greater than 3×10^8 dyn/cm^2 (McIntosh and Simon, 1994). In addition, Untracht and Shipley (1977) found that equimolar SM and eggPC formed separate phases in excess water, whereas for 3:1 and 2:1 eggPC:SM phase separation was observed at lower water contents.

As shown in Fig. 3, for 1:1:1 DOPC:SM:cholesterol the lamellar repeat (*d*) decreased monotonically with increasing osmotic pressure, from the maximal value of 67.6 Å with no applied pressure to 54.1 Å at an applied pressure of 5.9×10^8 dyn/cm^2 (log $P = 8.8$). Osmotic stress/x-ray experiments were also performed on DSMs, DRMs, and lipid preparations with compositions similar to those found for DSMs (DOPC and 2:1 DOPC:cholesterol) and DRMs (2:1 SM:cholesterol). No lamellar diffraction was recorded for isolated DSMs over a range of osmotic pressures. The reason for this absence of lamellar diffraction is unknown, but is probably due to residual amounts of Triton X-100 in the specimens. However, lamellar diffraction patterns were recorded for isolated DRMs. The experiments reported below are for DRMs obtained with treatment with 1% Triton X-100, although patterns with almost identical spacings and intensity distributions were also obtained from DRMs obtained with 4% Triton X-100 treatment (data not shown). Over the entire range of applied osmotic pressures the repeat periods for the DRMs were very similar to those recorded for 2:1 SM:cholesterol (Fig. 3). For DOPC, 2:1 DOPC:cholesterol, 2:1 SM:cholesterol, or DRMs the repeat periods monotonically decreased with increasing osmotic pressure, as was the case for 1:1:1 DOPC:SM:cholesterol (Fig. 3). However, compared with the repeat periods for 1:1:1 DOPC:SM:cholesterol, for each value of osmotic pressure the repeat period was smaller for DOPC and 2:1 DOPC:cholesterol and larger for DRMs and for 2:1 SM:cholesterol.

The repeat periods in Fig. 3 correspond to the width of a unit cell, which contains the bilayer and the fluid spacing between adjacent bilayers. To determine the relative bilayer widths of DOPC, 2:1 DOPC:cholesterol, 1:1:1 DOPC:SM:

cholesterol, DRMs, and 2:1 SM:cholesterol, the osmotic stress data were analyzed by Fourier techniques (McIntosh and Simon, 1986; McIntosh and Holloway, 1987). As a first step, the structure factors for all of the x-ray/osmotic stress data (Fig. 3) that contained at least four orders of diffraction were plotted versus reciprocal spacing. The structure factors for 1:1:1 DOPC:SM:cholesterol, 2:1 SM:cholesterol, and 2:1 DOPC:cholesterol are shown in Fig. 4, *A*, *B*, and *C*, respectively. In each panel the solid line corresponds to the continuous Fourier transform calculated by use of the sampling theorem (Shannon, 1949). It can be seen that for each of these lipid systems the data points fell quite closely to the continuous transform, indicating that the structure of the bilayer did not appreciably change with increasing osmotic pressure (McIntosh and Simon, 1986; McIntosh et al., 1987). For comparison, the structure factors for the DRMs are shown in both Fig. 4, *B* and *C*. The DRM structure factors fell quite closely to the continuous Fourier transform of 2:1 SM:cholesterol (Fig. 4 *B*), but were significantly displaced from the transform of 2:1 DOPC:cholesterol (Fig. 4 *C*). This indicates that the structure of DRMs was similar to 2:1 SM:cholesterol but was quite different than 2:1 DOPC:cholesterol bilayers.

The structure factors were used to calculate electron density profiles across the bilayers. Fig. 5 compares electron density profiles for DRMs, 2:1 DOPC:cholesterol, and DOPC all calculated at the same resolution ($d/2h_{max} \approx 8$ Å). For each profile the center of the bilayer is located at the origin, the low electron density trough in the center of the profile corresponds to the terminal methyl groups at the ends of the hydrocarbon chains, the medium density regions on either side of this trough correspond to the methylene chain regions of the bilayer, and the high electron density peaks near the edge of the profile correspond to the lipid headgroups. Several structural features can be seen from these profiles and profiles obtained from the other osmotic stress data. First, the headgroup peak separations (d_{pp}) were nearly constant for the osmotic pressures shown in Fig. 3: 36.0 ± 1.0 Å ($n = 5$ experiments) for DOPC, 38.4 ± 0.5 Å ($n = 4$) for 2:1 DOPC:cholesterol, 43.0 ± 1.5 Å ($n = 6$) for 1:1:1 DOPC:SM:cholesterol, 47.8 ± 1.0 Å ($n = 8$) for 2:1 SM:cholesterol, 47.0 Å ± 1.2 Å ($n = 5$) for DRMs obtained from 1% Triton X-100, and 48.0 ± 0.5 Å ($n = 3$) for DRMs obtained from 4% Triton X-100. Second, as illustrated in Fig. 5, d_{pp} was significantly wider for DRMs (headgroup peaks are noted by vertical dotted lines) than for either 2:1 DOPC:cholesterol or DOPC (head group peaks noted by vertical dashed lines). Third, whereas the profile of DOPC featured a rather shallow terminal methyl trough in the center of the bilayer, the profiles for both DRMs and 2:1 DOPC:cholesterol had much sharper terminal methyl roughs and a somewhat higher electron density in the methylene region of the bilayer. This characteristic feature of profiles of phospholipid bilayers containing cholesterol is due to two factors: 1) cholesterol increases the order in the

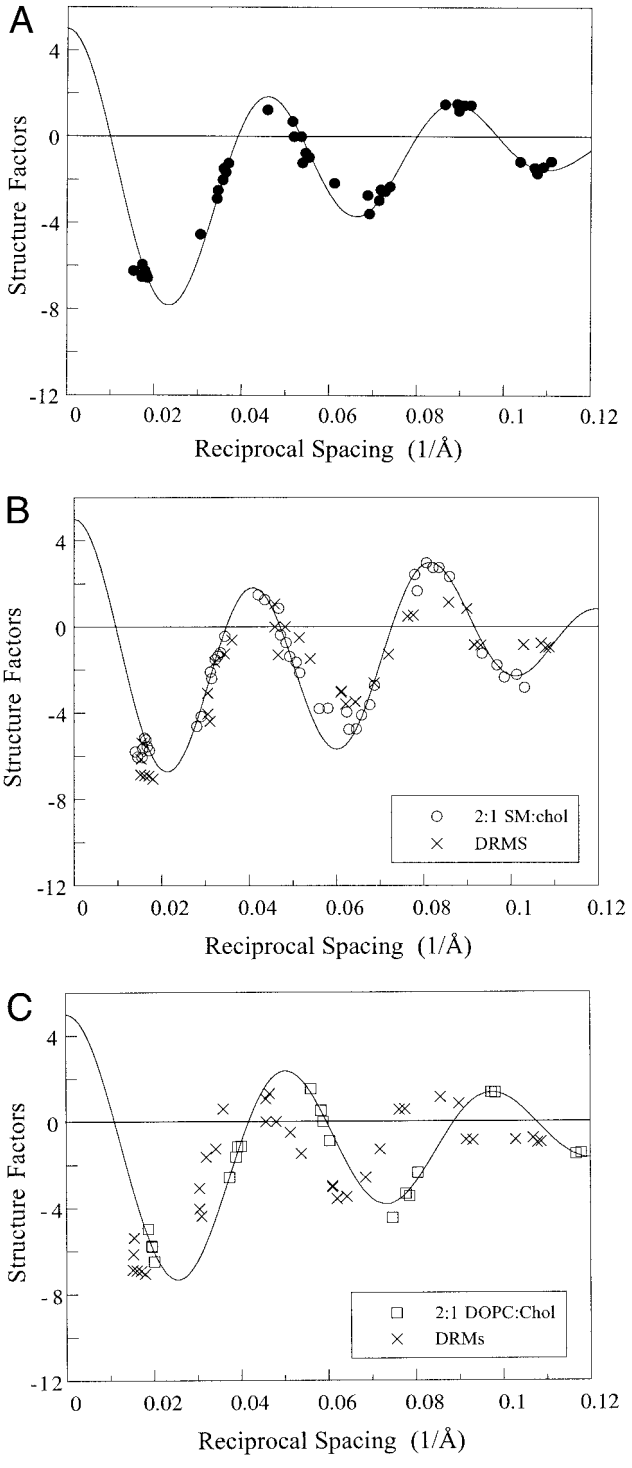

FIGURE 4 Structure factors plotted versus reciprocal spacing for osmotic stress/x-ray experiments of (*A*) 1:1:1 DOPC:SM:cholesterol, (*B*) 2:1 SM:cholesterol, and (*C*) 2:1 DOPC:cholesterol. In each panel the solid lines represent the continuous transform of the data calculated by use of the sampling theorem (Shannon, 1949). For comparison, the observed structure factors for DRMs are also included in *B* and *C*.

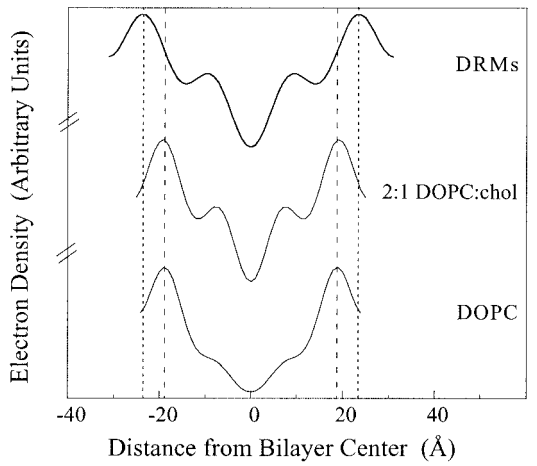

FIGURE 5 Electron density profiles (resolution of $d/2h_{max} \approx 8$ Å) for DRMs, 2:1 DOPC:cholesterol, and DOPC all at 79% relative humidity. For each profile, the center of the bilayer is at the origin and the high-density peaks (indicated with vertical dotted lines for DRMs and vertical dashed lines for DOPC) correspond to the lipid head groups.

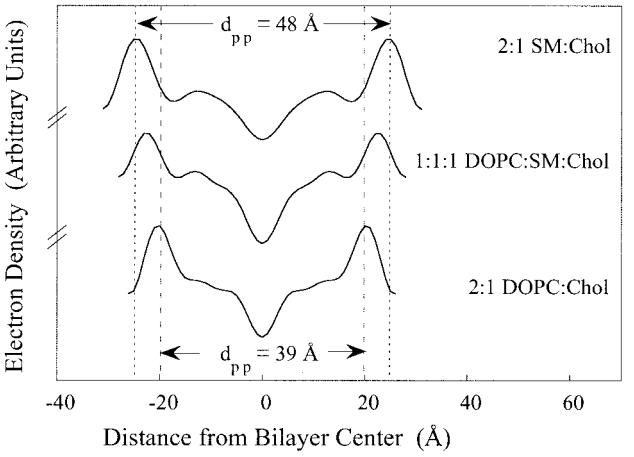

FIGURE 7 Electron density profiles (resolution of $d/2h_{max} \approx 4.5$ Å) for 2:1 SM:cholesterol, 1:1:1 DOPC:SM:cholesterol, and 2:1 DOPC:cholesterol. For each profile, the center of the bilayer is at the origin and the high-density peaks correspond to the lipid head groups. The headgroup peaks are noted with vertical dotted lines for 2:1 SM:cholesterol and with dashed lines for 2:1 DOPC:cholesterol.

hydrocarbon region, thereby localizing the terminal methyl groups in the center of the bilayer, and 2) the electron density of the cholesterol steroid rings is greater than the electron density of the phospholipid methylene chains (Franks, 1976; McIntosh, 1978; McIntosh et al., 1989a).

Fig. 6 compares electron density profiles at a resolution of $d/2h_{max} \approx 8$ Å for DRMs, 2:1 SM:cholesterol, and 1:1 SM:cholesterol. The distance between headgroup peaks and the shape of the profile was quite similar for the three profiles, indicating that the structure of the bilayer was similar for each system. The major difference among the profiles was that the methylene chain region of the bilayer had somewhat different electron densities, with the relative density of this region for the DRMs being between that of 1:1 SM:cholesterol and 2:1 SM:cholesterol. This was consistent with the biochemical analysis (Table 1) which found that DRMs had a SM:cholesterol ratio of 1.5:1.

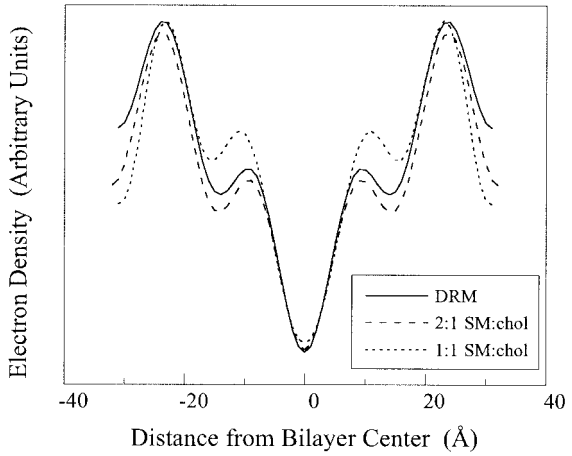

FIGURE 6 Electron density profiles (resolution of $d/2h_{max} \approx 8$ Å) for DRMs, 2:1 SM:cholesterol, and 1:1 SM:cholesterol. For each profile, the center of the bilayer is at the origin and the high-density peaks correspond to the lipid head groups.

Fig. 7 shows a comparison of electron density profiles at a higher resolution of $d/2h_{max} \approx 4.5$ Å for 2:1 SM:cholesterol, 1:1:1 DOPC:SM:cholesterol, and 2:1 DOPC:cholesterol. The vertical dotted and dashed lines denote the headgroup peaks for 2:1 SM:cholesterol and 2:1 DOPC:cholesterol, respectively. As measured by the peak-to-peak separation the 2:1 SM:cholesterol bilayer was ~9 Å wider than the 2:1 DOPC:cholesterol bilayers, consistent with the lower resolution data ($d/2h_{max} \approx 8$ Å) described above. The peak-to-peak separation of 1:1:1 DOPC:SM:cholesterol bilayers was approximately halfway between that of 2:1 SM:cholesterol and 2:1 DOPC:cholesterol bilayers.

The above values of d_{pp} can be used to estimate the fluid separation between bilayers as a function of osmotic pressure. Because the distance from the headgroup peak to the edge of the bilayer for PC or SM is ~5 Å (McIntosh and Simon, 1986; McIntosh et al., 1987, 1989a, 1992a), we estimate the total bilayer thickness as $d_b = d_{pp} + 10$ Å and determine the interbilayer fluid separation as $d_f = d - d_b$. Fig. 8 displays a plot of the pressure versus fluid separation for 2:1 DOPC:cholesterol, 1:1:1 DOPC:SM:cholesterol, 2:1 SM:cholesterol, and DRMs. For large osmotic pressures ($\log P > 7$), the fluid separations were similar for the four systems. However, in the absence of applied pressure (data points displayed on x axis), the fluid separation was ~4 Å larger for 2:1 DOPC:cholesterol than for 2:1 SM:cholesterol or the DRM, with the 1:1:1 DOPC:SM:cholesterol having an intermediate value of d_f.

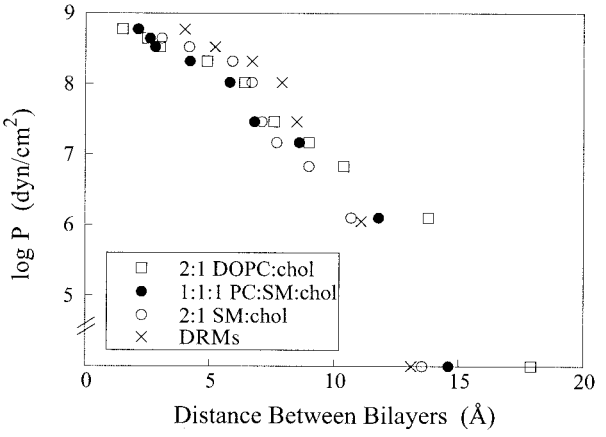

FIGURE 8 Plot of the logarithm of applied osmotic pressure versus the distance between bilayers for 2:1 DOPC:cholesterol, 1:1:1 DOPC:SM:cholesterol, 2:1 SM:cholesterol, and DRMs. Data from MLVs in water with no applied pressure are shown on the *x* axis.

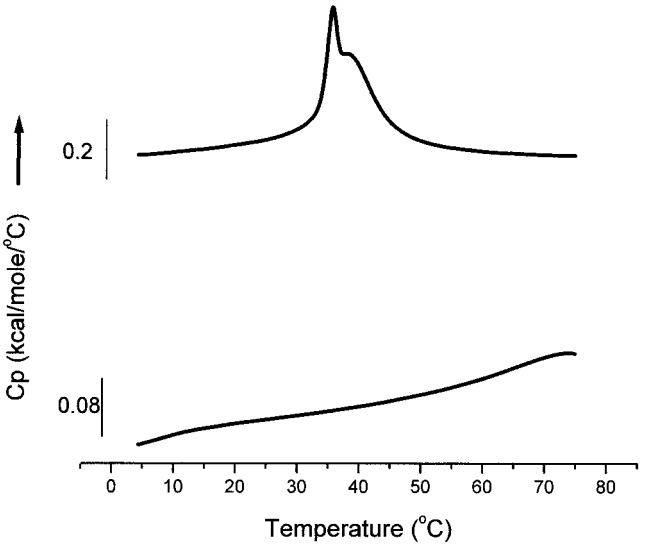

FIGURE 9 Thermograms showing the excess heat capacity versus temperature for lipid dispersions comprised of 83:17 DPPC:cholesterol (52 mg total) in 1 ml water (upper trace) and 1:1:1 DOPC:SM:cholesterol (123 mg total) in 1 ml water (lower trace). The large lipid concentration of the latter dispersion was used to optimize the detection of possible small enthalpy transitions. Note that bottom thermogram is shown on a more sensitive scale. The heating rate was 15°C/h. The arrow points in the direction of an endothermic transition.

Differential scanning calorimetry

As noted in the Introduction, it has been reported that giant unilamellar vesicles of equimolar DOPC:SM:cholesterol (that also contained 1 mol% GM1 and 0.5 mol% of the fluorescent probe LAURDAN) exhibit a reversible phase transition between 25 and 30°C (Dietrich et al., 2001). This transition is thought to represent the melting of rafts in a mixed liquid-ordered (L_o)/liquid-disordered (L_d) phase into a one-component L_d phase (no rafts). To test whether we can identify transitions between the L_o and L_d phases we first investigated the thermal behavior of DPPC bilayers containing 17 mol% cholesterol, a system that has a transition from gel phase to a mixed L_o-L_d phase at a temperature slightly below 40°C, as well as a transition from a mixed L_o-L_d to a pure L_d phase at a somewhat higher temperature, ~45°C (Ipsen et al., 1987). The thermogram for this system (Fig. 9) showed two transitions, a sharp endothermic transition with a peak at 38°C and a broader endothermic transition with a peak centered at 41°C. Although the transition temperatures were somewhat lower than expected from the phase diagram of Ipsen et al. (1987), the thermogram demonstrated the two expected transitions in that phase diagram with the higher temperature peak corresponding to the transition from a mixed L_o-L_d phase to a pure L_d phase. Similar DSC results have been obtained for DPPC bilayers containing a higher concentration of cholesterol (Epand et al., 2001). In contrast, thermograms of 1:1:1 DOPC:SM:cholesterol (Fig. 9) were featureless over the temperature range 3 to 75°C and did not demonstrate a transition in the region of between 25 and 30°C where a transition has been observed by fluorescence microscopy (Dietrich et al., 2001).

Peptide binding

We measured the binding of three peptides to single walled vesicles composed of DOPC, DOPC:cholesterol, and SM:cholesterol. One peptide, BR-C, is a 36 amino acid peptide equivalent to the third transmembrane helix in bacteriorhodopsin. At pH 5.5, BR-C partitions into bilayers in the form of a transbilayer helix (Hunt et al., 1997). For 5 μM peptide and 1.5 mM lipid at pH 5.5, the percent BR-C bound to LUVs was 57% to DOPC bilayers, 33% to bilayers of 2:1 DOPC:cholesterol, but only 5% bound to 2:1 SM:cholesterol and 6% bound to 1:1 SM:cholesterol. Thus, a larger percentage of this transmembrane peptide bound to DSMs than to DRMs.

We also measured the binding of two amphipathic peptides (MPR and melittin) that partition primarily into the bilayer interface (Altenbach et al., 1989; Hammen et al., 1996; Ghosh et al., 1997). For 5 μM peptide and 1.5 mM lipid in the form of SUVs the percent MPR bound was 40% to DOPC bilayers, 30% to 2:1 DOPC:cholesterol, 18% to 2:1 SM:cholesterol, and 7% to 1:1 SM:cholesterol. For LUVs the binding of MPR was 11% to DOPC, whereas no detectable binding was observed to 1:1 SM:cholesterol. Thus, for both SUVs and LUVs a greater percentage of this amphipathic peptide bound to bilayers with the composition of DSMs than to bilayers with the composition of DRMs. A similar phenomenon was observed with the amphipathic peptide melittin; using 10 μM peptide and 0.1 mM lipid we found the percent melittin bound was 52% to DOPC SUVs

TABLE 2 Mole fraction partition coefficients (K_p) for amphipathic peptides and SUVs

Lipid	MPR (SUVs)	MPR (LUVs)	Melittin (SUVs)	Melittin (LUVs)
DOPC	3.6×10^4	9.3×10^3	9.1×10^5	4.6×10^5
2:1 DOPC:cholesterol	2.4×10^4	—	—	—
2:1 SM:cholesterol	1.2×10^4	—	—	—
1:1 SM:cholesterol	3.9×10^3	ND	2.5×10^4	9.7×10^3

and 3% to 1:1 SM:cholesterol SUVs, and 29% to DOPC LUVs and less than 1% to 1:1 SM:cholesterol LUVs. For both of these peptides these binding percentages were converted into mole fraction partition coefficients (K_p) that are displayed in Table 2. For both peptides K_p was an order of magnitude higher for bilayers of DOPC than for bilayers of 1:1 SM:cholesterol, indicating that both of these amphipathic peptides bound to a greater extent to DSMs than to DRMs.

DISCUSSION

The data presented in this paper provide detailed information on the composition, structure, interbilayer interactions, and peptide-bilayer interactions of detergent resistant and detergent soluble membranes isolated from DOPC:SM:cholesterol bilayers.

Composition of DSMs and DRMs

Our chemical assays of DRMs and DSMs isolated from equimolar DOPC:SM:cholesterol bilayers show that the DRMs were enriched in SM and cholesterol, consistent with chemical assays of DRMs from both liposomes (Schroeder et al., 1994) and biological membranes (Hanada et al., 1995; Liu et al., 1997; Fridriksson et al., 1999; London and Brown, 2000; MacDonald, 1980; Prinetti et al., 2000; Gkantiragas et al., 2001). This suggests that cholesterol-lipid interactions are involved in raft formation in membranes containing SM. In terms of mechanism, Li et al. (2001) found that the detergent solubility of phospholipid:cholesterol mixtures depended on acyl chain and interfacial group composition and argued that these features in naturally occurring SM make SM:cholesterol bilayers resistant to solubilization by detergents.

Structure of DSMs and DRMs

The wide-angle x-ray diffraction data show that DRMs and the total 1:1:1 DOPC:SM:cholesterol bilayers were in the physiologically relevant liquid-crystalline phase. At present, the types of liquid-crystalline phases (liquid-disordered and liquid-ordered (Ipsen et al., 1987)) cannot be distinguished by wide-angle x-ray patterns. However, the x-ray patterns do show that there was no gel phase present in any of these cholesterol-containing systems. This conclusion is consistent with recent studies of domain formation in planar bilayers containing SM, cholesterol, DOPC, and dioleoylphosphatidylethanolamine (DOPE) (Samsonov et al., 2001).

Both the structure factor data (Fig. 4, *B* and *C*) and the electron density profiles (Figs. 5–7) showed that DRM bilayers had quite similar structures to 2:1 SM:cholesterol bilayers, but different structures than DOPC or 2:1 DOPC:cholesterol bilayers. Specifically, the bilayer thickness was, within experimental uncertainty, the same for DRMs and 2:1 SM:cholesterol, whereas the DRM bilayers were 9 and 11 Å wider than 2:1 DOPC:cholesterol and DOPC bilayers, respectively. These values were larger than the height difference of 4 Å observed by AFM between two phases in 1:1:1 DOPC:SM:cholesterol supported bilayers (Rinia et al., 2001). However, it is difficult to make direct comparisons between MLV bilayers and supported bilayers, particularly in the case of bilayers with uneven surfaces, such as bilayers with domains. According to Rinia et al. (2001), one would expect all of the lipid headgroups on the supported side of the bilayer to adhere to the flat mica surface. This would prevent the anchored monolayer from bending, and could affect the energetics of lipid self-association and the interaction between domains in apposing monolayers.

Relevance of DRM and DSM widths to protein sorting in cells

The electron density profiles (Figs. 5 and 6) provide estimates for the relative thicknesses of raft and nonraft membrane bilayers in typical plasma membranes. A complicating feature of this analysis is that in biological membranes it is not known whether rafts are present in monolayers or bilayers, although current models depict bilayer rafts (Simons and Ikonen, 2000; Galbiati et al., 2001). In principle, the DRMs obtained in these experiments should have a similar lipid composition to the SM:cholesterol rafts found in plasma membranes since the SM used here was isolated from brain membranes. Either DOPC or 2:1 DOPC:cholesterol are a reasonable model for the nonraft bilayers in plasma membranes. However, in plasma membranes there are often a variety of phospholipids with differences in hydrocarbon chain length and degree of unsaturation, and the bilayer width depends on both of those factors (Lewis and Engelman, 1983). We have measured the peak-to-peak separation (d_{pp}) for a variety of bilayers. Compared with the d_{pp} values of 36.0 Å for DOPC and 38.4 Å for 2:1 DOPC:cholesterol, we found $d_{pp} = 37.8$ Å for eggPC (McIntosh and Simon, 1986) (a natural product containing a mixture of hydrocarbon chains), $d_{pp} = 40.2$ Å for 2:1 eggPC:cholesterol (McIntosh et al., 1989a), and $d_{pp} = 40.7$ Å for (C18:0)(C18:1)PC (Rawicz et al., 2000). Thus, for representative nonraft lipid bilayers d_{pp} ranges between 36 and 41 Å, compared with $d_{pp} = 47$ Å for DRMs. Therefore, for typical

plasma membranes containing lipids with a mixture of hydrocarbon chains, and with the assumption that rafts involve the entire bilayer, our measurements indicate that the width of a nonraft bilayer should be 6 to 11 Å smaller than that of the raft bilayer.

These estimates for the widths of raft and nonraft bilayers have relevance to models of protein sorting in the Golgi due to matching of the length of the hydrophobic transmembrane domains of proteins with the lipid bilayer thickness (Bretscher and Munro, 1993; Munro, 1995). The length of the average transmembrane segment is ~15 amino acid residues for resident Golgi proteins and ~20 amino acids for plasma membrane proteins (Bretscher and Munro, 1993). Therefore, because an α helix has a length of ~1.5 Å per amino acid residue, the transmembrane segments of resident Golgi proteins are, on average, ~7.5 Å shorter than those of plasma membranes. This distance is within the range of our estimated difference between the widths of DSMs and DRMs. Thus, our results for bilayer thicknesses of DSMs and DRMs are consistent with models of lipid-based sorting of proteins based on hydrophobic matching (Bretscher and Munro, 1993; Munro, 1995). However, as described below, other factors, such as the difference in mechanical properties of DSMs and DRMs, could effect the distribution of proteins within membranes.

Domain formation: role of cholesterol

These x-ray data provide information relevant to domain formation in lipid bilayer systems. The patterns in Fig. 2 show that cholesterol tends to prevent the phase separation typically found in mixtures of gel and liquid-crystalline bilayers. The addition of cholesterol to a mixture of gel phase SM and liquid-crystalline phase DOPC produces multilayers that are completely liquid-crystalline and have a single repeat period. This means that each MLV in the dispersion has a similar structure. This change in phase properties caused by the addition of cholesterol is consistent with the phase diagram of Feigenson and Buboltz (2001) for mixtures of cholesterol with gel phase DPPC (16 carbons per acyl chain) and liquid-crystalline phase dilauroylphosphatidylcholine (DLPC, 12 carbons per chain). With fluorescence light microscopy study, Feigenson and Buboltz (2001) have demonstrated that, although there are coexisting DLPC-enriched fluid and DPPC-enriched ordered phases at low cholesterol concentrations, cholesterol concentrations greater than 25 mol% produce a single bilayer phase, independent of the relative concentrations of DPPC or DLPC.

Osmotic stress/x-ray diffraction experiments are particularly useful for detecting possible phase separations. Large osmotic pressures promote phase separation because the pressure causes the area per lipid molecule to decrease (Parsegian et al., 1979; Parsegian and Rand, 1983; McIntosh et al., 1987), forcing lipids to maximize their van der Waals interactions. Even at high osmotic pressures 1:1:1 DOPC:SM:cholesterol showed only one repeat period (Fig. 3). Therefore we conclude that 1:1:1 DOPC:SM:cholesterol bilayers do not exhibit three-dimensional phase separations.

Previous experiments using fluorescence microscopy (Dietrich et al., 2001), AFM (Rinia et al., 2001), and fluorescence quenching (Ahmed et al., 1997) have indicated the presence of lipid domains with the same equimolar DOPC:SM:cholesterol system studied in this paper, and Samsonov et al. (2001) observed domains in planar bilayers formed from squalene and containing DOPC, DOPE, SM, and cholesterol. We now consider the apparent differences between our results, which show no evidence of three-dimensional phase separation in DOPC:SM:cholesterol bilayers, and these previous studies, which show the presence of bilayer domains. The quenching curves of Ahmed et al. (1997), also performed on MLVs, do not provide information on the lateral size of the phase-separated domains and small domains would not be detected by the low-angle x-ray experiments. Thus, the quenching and x-ray data are consistent, particularly if the domains were relatively small.

The results of Dietrich et al. (2001), Rinia et al. (2001), and Samsonov et al. (2001), which show micron-sized domains, are perhaps more difficult to correlate with our x-ray and DSC results. There are at least two possible reasons why domains are visualized in supported bilayers (Dietrich et al., 2001; Rinia et al., 2001), planar bilayers (Samsonov et al., 2001), and GUVs (Dietrich et al., 2001), but not detected in MLVs by lamellar x-ray diffraction. One possibility involves differences in the preparations. As noted above, supported bilayers have quite different boundary conditions than MLVs. Planar bilayers, in equilibrium with a torus of squalene, also have different boundary conditions than MLVs, and the planar bilayers studied by Samsonov et al. (2001) had a different lipid composition as they contained DOPE. Although GUVs would appear to be a more similar system to MLVs, it should be noted that the DLPC:DPPC:cholesterol GUVs studied by Feigenson and Buboltz (2001), where fluorescence microscopy showed only a single region (no domains) at high cholesterol concentrations, were made by a different procedure (Akashi et al., 1996), than the "electroformation" method used by Dietrich et al. (2001). A second possible explanation for the observed differences is that a critical feature for the x-ray experiments is the manner in which apposing 1:1:1 DOPC:SM:cholesterol bilayers stack together to form three-dimensional multilayers. If micron-sized raft domains stacked together in three dimensions, one would expect to see a repeat period similar to that of DRMs (as well as a smaller repeat period if the DSM bilayers stacked together), rather than the observed repeat period that is midway between that of DRMs and DSMs (Fig. 3). However, one might not detect the presence of large domains, even at high osmotic pressures, if during multilayer formation the wide bilayer domains stacked against the narrow bilayer domains from apposing

bilayers, as in stacked egg cartons. In that case the x-ray patterns would reflect the average spacing of the two domains, as indeed they do (Fig. 3).

In terms of thermal properties, even though we used large lipid concentrations and a sensitive calorimeter, we were not able to detect a phase transition in DOPC:SM:cholesterol (Fig. 9) at temperatures where structural changes were observed (Dietrich et al., 2001; Samsonov et al., 2001). Presumably the transitions observed by Dietrich et al. (2001) and Samsonov et al. (2001) represent a transition between a two-phase (liquid-ordered/liquid disordered) region and a single liquid-disordered phase, similar to the higher temperature transition observed in our control experiments with DPPC:cholesterol (Fig. 9). There are several possible reasons why phase transitions are observed by microscopy in GUVs (Dietrich et al., 2001) and planar bilayers (Samsonov et al., 2001), but not by DSC in MLVs. The first is that the transition is simply not present in equimolar DOPC:SM:cholesterol MLVs. A second possibility is the differences in boundary conditions between planar bilayers, GUVs, and MLVs described in the previous paragraph can change the chemical potential of the various components. A third possibility, and the one that we favor, is that there is a transition, but that the heat absorbed by this transition is too small to be detected as a peak by DSC. The transition might rather appear like a second order phase transition with a more gradual change in heat capacity. In any event, the transition enthalpy under a peak is expected to be critically dependent on the amount of cholesterol in the DRM. Previous studies of SM:cholesterol thermal properties, using bovine brain SM (McIntosh et al., 1992b) and *N*-palmitoylsphingomyelin (Calhoun and Shipley, 1979a,b), showed that there is a broad transition with an enthalpy of ~1 kcal/mol for 2:1 SM:cholesterol, but no detectable transition for 1:1 SM:cholesterol. Thus, with the assumption that there indeed is a transition in 1:1:1 DOPC:SM:cholesterol, the DSC data indicate, in agreement with the results in Table 1 and Fig. 6, that cholesterol must be highly enriched in the DRMs.

Interbilayer interactions

The pressure-distance data obtained for 1:1:1 DOPC:SM:cholesterol bilayers (Fig. 8) were similar to those previously obtained for other liquid-crystalline bilayer systems. That is, for pressures greater than 10^6 dyn/cm^2 (log $P = 6$) the data points can be closely fit (least squares fit with $R^2 = 0.985$) to an exponential function of the form

$$P(d_f) = P_0 \exp(-d_f/\lambda) \quad (3)$$

with a decay length $\lambda = 1.6$ Å. Over this pressure range this decay length was similar to that previously found for a variety of uncharged liquid-crystalline bilayer systems, including PC, PC:cholesterol, and SM:cholesterol (LeNeveu et al., 1977; Parsegian et al., 1979; McIntosh and Simon, 1986; Rand and Parsegian, 1989; McIntosh et al., 1992a).

The 2:1 DOPC:cholesterol and 2:1 SM:cholesterol data were close to the 1:1:1 DOPC:SM:cholesterol data for pressures greater than 10^6 dyn/cm^2 (Fig. 8). However, for log $P < 6$ the fluid spacing for 2:1 DOPC:cholesterol was greater than d_f for 2:1 SM:cholesterol. In particular, in the absence of applied pressure (data shown on the x axis) the fluid spacing was over 4 Å larger for 2:1 DOPC:cholesterol than for 2:1 SM:cholesterol. A likely explanation for this difference is that the repulsive undulation pressure (Harbich and Helfrich, 1984; Evans and Parsegian, 1986; McIntosh et al., 1989b; Evans, 1991) is larger for 2:1 DOPC:cholesterol than for 2:1 SM:cholesterol due to the larger bilayer bending modulus and smaller compressibility modulus for the former bilayers (Needham and Nunn, 1990; McIntosh et al., 1992a). Experimental studies have shown that the undulation pressure increases d_f at low applied pressures (McIntosh and Simon, 1993; McIntosh et al., 1995).

Peptide binding of DSMs and DRMs

More of the transmembrane peptide BR-C partitioned into DOPC or DOPC:cholesterol bilayers than into SM:cholesterol bilayers. There are at least two possible reasons for this difference: 1) the transbilayer width of BR-C matches more closely with the hydrocarbon thickness of DOPC than SM:cholesterol or 2) the larger area compressibility modulus of SM:cholesterol (Needham and Nunn, 1990) compared with DOPC would mean that more energy would be needed to separate the acyl chains and therefore would make it energetically unfavorable for the peptide to partition into the SM:cholesterol bilayer. Although both factors might contribute, the partition coefficient data for MPR and melittin (Table 2) provide strong evidence in favor of the latter mechanism. Both MPR (Hammen et al., 1996) and melittin (Altenbach et al., 1989; Ghosh et al., 1997; Kleinschmidt et al., 1997) partition into the bilayer interfacial region and both these peptides had a larger partition coefficient for DOPC bilayers than for SM:cholesterol bilayers (Table 2). For these interfacial peptides differences in hydrocarbon thickness should not markedly affect partitioning, although differences in compressibility modulus would. Therefore, for DOPC and SM:cholesterol bilayers the difference in compressibility modulus, rather than the difference in hydrocarbon thickness, appears to be a more important factor in the binding of these particular peptides. Future directions involve determining whether peptides of different hydrophobic lengths can be sorted between DSMs and DRMs solely on the basis of differences in bilayer thickness.

This work was supported by grants GM27278 and GM58432 from the National Institutes of Health.

REFERENCES

Ahmed, S. N., D. A. Brown, and E. London. 1997. On the origin of sphingolipid/cholesterol-rich detergent-insoluble cell membranes: physiological concentrations of cholesterol and sphingolipid induce formation of a detergent-insoluble, liquid-ordered lipid phase in model membranes. *Biochemistry.* 36:10944–10953.

Akashi, K.-I., H. Miyata, H. Itoh, and K. Kinosita. 1996. Preparation of giant liposomes in physiological conditions and their characterization under an optical microscope. *Biophys. J.* 71:3242–3250.

Altenbach, C., W. Froncisz, J. S. Hyde, and W. L. Hubbell. 1989. Conformation of spin-labeled melittin at membrane surfaces investigated by pulse saturation recovery and continuous wave power saturation electron paramagnetic resonance. *Biophys. J.* 56:1183–1191.

Arreaza, G., and D. A. Brown. 1995. Sorting and intracellular trafficking of a glycosylphosphatidylinositol-anchored protein and two hybrid proteins with the same ectodomain in MDCK kidney epithelial cell. *J. Biol. Chem.* 270:23641–23647.

Babiychuk, E. B., and A. Draeger. 2000. Annexins in cell membrane dynamics: Ca2+-regulated association of microdomains. *J. Cell Biol.* 150:1113–1123.

Baird, B., E. D. Sheets, and D. Holowka. 1999. How does the plasma membrane participate in cellular signaling by receptors for immunoglobulin E? *Biophys. Chem.* 82:109–119.

Bretscher, M. S., and S. Munro. 1993. Cholesterol and the Golgi apparatus. *Science.* 261:1280–1281.

Brown, D. A., and E. London. 1998. Functions of lipid rafts in biological membranes. *Annu. Rev. Cell Dev. Biol.* 14:111–136.

Brown, D. A., and E. London. 2000. Structure and function of sphingolipid- and cholesterol-rich membrane rafts. *J. Biol. Chem.* 275: 17221–17224.

Buser, C. A., and S. McLaughlin. 1998. Ultracentrifugation techniques for measuring the binding of peptides and proteins to sucrose-loaded phospholipid vesicles. *Methods Mol. Biol.* 84:267–281.

Calhoun, W. I., and G. G. Shipley. 1979a. Fatty acid composition and thermal behavior of natural sphingomyelins. *Biochim. Biophys. Acta.* 555:436–441.

Calhoun, W. I., and G. G. Shipley. 1979b. Sphingomyelin-lecithin bilayers and interaction with cholesterol. *Biochemistry.* 18:1717–1722.

Chamberlain, L. H., R. D. Burgoyne, and G. W. Gould. 2001. SNARE proteins are highly enriched in lipid rafts in PC12 cells: implications for the spatial control of exocytosis. *Proc. Natl. Acad. Sci. U. S. A.* 98: 5619–5624.

Chen, P. S., Jr., T. Y. Toribara, and H. Warner. 1956. Microdetermination of phosphorous. *Anal. Chem.* 28:1756–1758.

dePlanque, M. R. R., E. Goormaghtigh, D. V. Greathouse, R. E. Koeppe, J. A. W. Kruijtzer, R. M. J. Kiskamp, D. deKruijff, and J. A. Killian. 2001. Sensitivity of single membrane-spanning α-helical peptides to hydrophobic mismatch with a lipid bilayer: effects on backbone structure, orientation, and extent of membrane incorporation. *Biochemistry.* 40:5000–5010.

Dietrich, C., L. A. Bagatolli, Z. N. Volovyk, N. L. Thompson, M. Levi, K. Jacobson, and E. Gratton. 2001. Lipid rafts reconstituted in model membranes. *Biophys. J.* 80:1417–1428.

Edidin, M. 1998. Lipid microdomains in cell surface membranes. *Curr. Opin. Struct. Biol.* 7:528–532.

Epand, R. M., S. Maekawa, C. M. Yip, and R. F. Epand. 2001. Protein-induced formation of cholesterol-rich domains. *Biochemistry.* 40: 10514–10521.

Evans, E. 1991. Entropy-driven tension in vesicle membranes and unbinding of adherent vesicles. *Langmuir.* 7:1900–1908.

Evans, E. A., and V. A. Parsegian. 1986. Thermal-mechanical fluctuations enhance repulsion between bimolecular layers. *Proc. Natl. Acad. Sci. U.S.A.* 83:7132–7136.

Faucon, J. F., J. Dufourcq, and C. Lussan. 1979. The self-association of melittin and its binding to lipids: an intrinsic fluorescence polarization study. *FEBS Lett.* 102:187–190.

Feigenson, G. W., and J. T. Buboltz. 2001. Ternary phase diagram of dipalmitoyl-PC/dilauroyl-PC/cholesterol: nanoscopic domain formation driven by cholesterol. *Biophys. J.* 80:2775–2788.

Field, K. A., D. Holowka, and B. Baird. 1997. Compartmentalized activation of the high affinity immunoglubulin E receptor within membrane domains. *J. Biol. Chem.* 272:4276–4280.

Foger, N., R. Marhaba, and M. Zoiler. 2001. Involvement of CD44 in cytoskelton rearrangement and raft reorganization in T cells. *J. Cell Sci.* 114:1169–1178.

Franks, N. P. 1976. Structural analysis of hydrated egg lecithin and cholesterol bilayers: I. X- ray diffraction. *J. Mol. Biol.* 100:345–358.

Fridriksson, E. K., P. A. Shipkova, E. D. Sheets, D. Holowka, B. Baird, and F. W. McLafferty. 1999. Quantitative analysis of phospholipids in functionally important membrane domains from RBL-2H3 mast cells using tandem high-resolution mass spectrometry. *Biochemistry.* 38: 8056–8063.

Galbiati, F., B. Razani, and M. P. Lisanti. 2001. Emerging themes in lipid rafts and caveolae. *Cell.* 106:403–411.

Gheber, L. A., and M. Edidin. 1999. A model for membrane patchiness: lateral diffusion in the presence of barriers and vesicle traffic. *Biophys. J.* 77:3163–3175.

Ghosh, A. K., R. Rukmini, and A. Chattopadhyay. 1997. Modulation of tryptophan environment in membrane-bound melittin by negatively charged phospholipids: implications in membrane organization and function. *Biochemistry.* 36:14291–14305.

Gkantiragas, I., B. Brugger, E. Stuven, D. Kaloyanova, X.-Y. Li, K. Lohr, F. Lottspeich, F. T. Wieland, and J. B. Helms. 2001. Sphingomyelin-enriched microdomains at the Golgi complex. *Mol. Biol. Cell.* 12: 1819–1833.

Hammen, P. K., D. G. Gorenstein, and H. Weiner. 1996. Amphilicity determines binding properties of three mitochondrial presequences to lipid surfaces. *Biochemistry.* 35:3772–3781.

Hanada, K., M. Nishijima, Y. Akamatsu, and R. E. Pagano. 1995. Both sphingolipids and cholesterol participate in the detergent insolubility of alkaline-phosphatase, a glycosylphosphatidylinositol-anchored protein, in mammalian membranes. *J. Biol. Chem.* 270:6254–6260.

Harbich, W., and W. Helfrich. 1984. The swelling of egg lecithin in water. *Chem. Phys. Lipids.* 36:39–63.

Harder, T., P. Scheiffele, P. Vekade, and K. Simons. 1998. Lipid domain structure of the plasma membrane revealed by patching of membrane components. *J. Cell Biol.* 141:929–942.

Hope, M. J., M. B. Bally, G. Webb, and P. R. Cullis. 1985. Production of large unilamellar vesicles by a rapid extrusion procedure. *Biochim. Biophys. Acta.* 812:55–65.

Hunt, J. F., P. Rath, K. J. Rothschild, and D. M. Engleman. 1997. Spontaneous, pH-dependent membrane insertion of a transbilayer α-helix. *Biochemistry.* 36:15177–15192.

Huttner, W. B., and J. Zimmerberg. 2001. Implications of lipid microdomains for membrane curvature, budding and fission. *Curr. Opin. Cell Biol.* 13:478–484.

Ikonen, E. 2001. Roles of lipid rafts in membrane transport. *Curr. Opin. Cell Biol.* 13:470–477.

Ipsen, J. H., G. Karlstrom, O. G. Mouritsen, H. Wennerstrom and M. J. Zuckermann. 1987. Phase equilibria in the PC-cholesterol system. *Biochim. Biophys. Acta.* 905:162–172.

Kates, M. 1972. Techniques of Lipidology: Isolation, Analysis and Identification of Lipids. North-Holland Publishing Company, Amsterdam.

Kawabuchi, M., Y. Satomi, T. Takao, Y. Shimonishi, S. Nada, K. Nagai, A. Tarakhovsky, and M. Okada. 2000. Transmembrane phosphoprotein Chp regulates the activity of Src-family of tyrosine kinase. *Nature.* 404:999–1003.

Kenworthy, A. K., and M. Edidin. 1998. Distribution of glycosylphosphatidylinositol-anchored protein at the apical surface of MDCK cells examined at a resolution of $<$100 Å using imaging fluorescence resonance energy transfer. *J. Cell Biol.* 142:69–84.

Kenworthy, A. K., N. Petranova, and M. Edidin. 2000. High-resolution FRET microscopy of cholera toxin B-subunit and GPI-anchored proteins in cell plasma membranes. *Mol Biol. Cell.* 11:1645–1655.

Killian, J. A. 1998. Hydrophobic mismatch between proteins and lipids in membranes. *Biochim. Biophys. Acta.* 1376:401–416.

Kleinschmidt, J. H., J. E. Mahaney, D. D. Thomas, and D. Marsh. 1997. Interaction of bee venom melittin with zwitterionic and negatively charged phospholipid bilayers: a spin-label electron spin resonance study. *Biophys. J.* 72:767–778.

Kulkarni, K., D. S. Snyder, and T. J. McIntosh. 1999. Adhesion between cerebroside bilayers. *Biochemistry.* 38:15264–15721.

Ladokhin, A. S., M. E. Selsted, and S. H. White. 1997. Bilayer interactions of indolicidin, a small antimicrobial peptide rich in tryptophan, proline, and basic amino acids. *Biophys. J.* 72:794–805.

Lafont, F., P. Verkade, T. Galli, C. Wimmer, D. Louvard, and K. Simons. 1999. Raft association of SNAP receptors acting in apical trafficking in Madin-Darby canine kidney cells. *Proc. Natl. Acad. Sci. U.S.A.* 96: 3734–3738.

Lang, T., D. Bruns, D. Wenzel, D. Riedel, P. Holroyd, C. Thiele, and R. Jahn. 2001. SNAREs are concentrated in cholesterol-dependent clusters that define docking and fusion sites for exocytosis. *EMBO J.* 20: 2202–2213.

LeNeveu, D. M., R. P. Rand, V. A. Parsegian, and D. Gingell. 1977. Measurement and modification of forces between lecithin bilayers. *Biophys. J.* 18:209–230.

Lewis, B. A., and D. M. Engelman. 1983. Lipid bilayer thickness varies linearly with acyl chain length in fluid phosphatidylcholine vesicles. *J. Mol. Biol.* 166:211–217.

Li, X.-M., M. M. Momsen, J. Smaby, H. L. Brockman, and R. E. Brown. 2001. Cholesterol decreases the interfacial elasticity and detergent solubility of sphingomyelins. *Biochemistry.* 40:5954–5963.

Liu, J., P. Oh, T. Horner, R. A. Rogers, and J. E. Schnitzer. 1997. Organized endothelial cell surface signal transduction in caveolae distinct from GPI-anchored protein microdomains. *J. Biol. Chem.* 272: 7211–7222.

London, E., and D. A. Brown. 2000. Insolubility of lipids in Triton X-100: physical origin and relationship to sphingolipid/cholesterol membrane domains (rafts). *Biochim. Biophys. Acta.* 1508:182–195.

MacDonald, R. I. 1980. Action of detergents on membranes: differences between lipid extracted from red cell ghosts and from red cell lipid vesicles by Triton X-100. *Biochemistry.* 19:1916–1922.

McIntosh, T. J. 1978. The effect of cholesterol on the structure of phosphatidylcholine bilayers. *Biochim. Biophys. Acta.* 513:43–58.

McIntosh, T. J., S. Advani, R. E. Burton, D. V. Zhelev, D. Needham, and S. A. Simon. 1995. Experimental tests for protrusion and undulation pressures in phospholipid bilayers. *Biochemistry.* 34:8520–8532.

McIntosh, T. J., and P. W. Holloway. 1987. Determination of the depth of bromine atoms in bilayers formed from bromolipid probes. *Biochemistry.* 26:1783–1788.

McIntosh, T. J., A. D. Magid, and S. A. Simon. 1987. Steric repulsion between phosphatidylcholine bilayers. *Biochemistry.* 26:7325–7332.

McIntosh, T. J., A. D. Magid, and S. A. Simon. 1989a. Cholesterol modifies the short-range repulsive interactions between phosphatidylcholine membranes. *Biochemistry.* 28:17–25.

McIntosh, T. J., A. D. Magid, and S. A. Simon. 1989b. Repulsive interactions between uncharged bilayers: hydration and fluctuation pressures for monoglycerides. *Biophys. J.* 55:897–904.

McIntosh, T. J., and S. A. Simon. 1986. The hydration force and bilayer deformation: a reevaluation. *Biochemistry.* 25:4058–4066.

McIntosh, T. J., and S. A. Simon. 1993. Contribution of hydration and steric (entropic) pressures to the interaction between phosphatidylcholine bilayers: experiments with the subgel phase. *Biochemistry.* 32: 8374–8384.

McIntosh, T. J., and S. A. Simon. 1994. Long- and short-range interactions between phospholipid/ganglioside GM1 bilayers. *Biochemistry.* 33: 10477–10486.

McIntosh, T. J., S. A. Simon, J. C. Ellington, and N. A. Porter. 1984. A new structural model for mixed-chain phosphatidylcholine bilayers. *Biochemistry.* 23:4038–4044.

McIntosh, T. J., S. A. Simon, D. Needham, and C.-H. Huang. 1992a. Interbilayer interactions between sphingomyelin and sphingomyelin: cholesterol bilayers. *Biochemistry.* 31:2020–2024.

McIntosh, T. J., S. A. Simon, D. Needham, and C.-H. Huang. 1992b. Structure and cohesive properties of sphingomyelin:cholesterol bilayers. *Biochemistry.* 31:2012–2020.

Melkonian, K. A., A. G. Ostermeyer, J. Z. Chen, M. G. Roth, and D. A. Brown. 1999. Role of lipid modifications in targeting proteins to detergent-resistant membrane rafts. Many raft proteins are acylated, while few are prenylated. *J. Biol. Chem.* 274:3910–3917.

Moffett, S., D. A. Brown, and M. E. Linder. 198. 2000. Lipid-dependent targeting of G proteins into rafts. *J. Biol. Chem.* 275:2191–2192.

Munro, S. 1995. An investigation of the role of transmembrane domains in Golgi protein retention. *EMBO J.* 14:4695–4704.

Needham, D., and R. S. Nunn. 1990. Elastic deformation and failure of lipid bilayer membranes containing cholesterol. *Biophys. J.* 58: 997–1009.

Oliferenko, S., K. Paiha, T. Harder, V. Gerke, C. Schwarzler, H. Schwarz, H. Beug, U. Gunthert, and L. Huber. 1999. Analysis of CD44-containing lipid rafts: recruitment of annexin II and stabilization by the actin cytoskeleton. *J. Cell Biol.* 146:843–854.

Parsegian, V. A., N. Fuller, and R. P. Rand. 1979. Measured work of deformation and repulsion of lecithin bilayers. *Proc. Natl. Acad. Sci. U.S.A.* 76:2750–2754.

Parsegian, V. A., and R. P. Rand. 1983. Membrane interaction and deformability. *Ann. N.Y. Acad. Sci.* 416:1–12.

Parsegian, V. A., R. P. Rand, N. L. Fuller, and R. C. Rau. 1986. Osmotic stress for the direct measurement of intermolecular forces. *Methods Enzymol.* 127:400–416.

Prinetti, A., V. Chigorno, G. Tettamanti, and S. Sonnino. 2000. Sphingolipid-enriched membrane domains from rat cerebellar granule cells differentiated in culture, a compositional study. *J. Biol. Chem.* 275: 11658–11665.

Quay, S. C., and C. C. Condie. 1983. Conformational studies of aqueous melittin: thermodynamic parameters of monomer-tetramer self-assocation reaction. *Biochemistry.* 22:695–700.

Rand, R. P., and V. A. Parsegian. 1989. Hydration forces between phospholipid bilayers. *Biochim. Biophys. Acta.* 988:351–376.

Rawicz, W., K. C. Olbrich, T. J. McIntosh, D. Needham, and E. Evans. 2000. Effect of chain length and unsaturation on elasticity of lipid bilayers. *Biophys. J.* 79:328–339.

Ren, J., S. Lew, J. Wang, and E. London. 1999. Control of the transmembrane orientation and interhelical interactions within membranes by hydrophobic helix length. *Biochemistry.* 38:5905–5912.

Rinia, H. A., M. M. E. Snel, J. P. J. M. van der Eerden, and B. deKruijff. 2001. Visualizing detergent resistant domains in model membranes with atomic force microscopy. *FEBS Lett.* 501:92–96.

Rodgers, W., B. Crise, and J. K. Rose. 1994. Signals determining protein tyrosine kinase and glycosyl-phosphatidylinositol-anchored proteins targeting to a glycolipid-enriched membrane fraction. *Mol. Cell Biol.* 14:5384–5391.

Samsonov, A. V., I. Mihalyov, and F. S. Cohen. 2001. Characterization of cholesterol-sphingomyelin domains and their dynamics in bilayer membranes. *Biophys. J.* 81:1486–1500.

Scheiffele, P., M. G. Roth, and K. Simons. 1997. Interaction of influenza virus hemagglutinin with sphingolipid-cholesterol membrane domains via it transmembrane domain. *EMBO J.* 16:5501–5508.

Schroeder, R., E. London, and D. Brown. 1994. Interactions between saturated acyl chains confer detergent resistance on lipids and glycosylphosphatidylinositol (GPI)-anchored proteins: GPI-anchored proteins in liposomes and cells show similar behavior. *Proc. Natl. Acad. Sci. U.S.A.* 91:12130–12134.

Schutz, G. J., G. Kada, V. P. Pastushenko, and H. Schindler. 2000. Properties of lipid microdomains in a muscle cell membrane visualized by single molecule microscopy. *EMBO J.* 19:892–901.

Shannon, C. E. 1949. Communication in the presence of noise. *Proc. Inst. Radio Engrs. N.Y.* 37:10–21.

Sheets, E. D., K. Jacobson, R. Simson, and G. M. Lee. 1997. Transient confinement of a glycosylphosphatidylinositol-anchored protein in the plasma membrane. *Biochemistry.* 36:12449–12458.

Simons, K., and E. Ikonen. 1997. Functional rafts in cell membranes. *Nature.* 387:569–572.

Simons, K., and E. Ikonen. 2000. How cells handle cholesterol. *Science.* 290:1721–1726.

Simons, K., and G. van Meer. 1988. Lipid sorting in epithelial cells. *Biochemistry.* 27:6197–6202.

Solomon, K. R., E. A. Kurt-Jones, R. A. Saladino, A. M. Stack, I. F. Dunn, M. Ferretti, D. Golenbock, G. R. Fleisher, and R. W. Finberg. 1998. Heterotrimeric G proteins physically associated with the lipopolysaccharide receptor CD14 modulate both in vivo and in vitro responses to lipopolysaccharide. *J. Clin. Invest.* 102:2019–2027.

Sophianopoulos, J. A., S. J. Durham, A. J. Sophianopoulos, H. L. Ragsdale, and W. P. Cropper. 1978. Ultrafiltration is theoretically equivalent to equilibrium dialysis but much simpler to carry out. *Arch. Biochem. Biophys.* 187:132–137.

Tang, Q., and M. Edidin. 2001. Vesicle trafficking and cell surface membrane patchiness. *Biophys. J.* 81:196–203.

Tardieu, A., V. Luzzati, and F. C. Reman. 1973. Structure and polymorphism of the hydrocarbon chains of lipids: a study of lecithin-water phases. *J. Mol. Biol.* 75:711–733.

Untracht, S. H., and G. G. Shipley. 1977. Molecular interactions between lecithin and sphingomyelin. *J. Biol. Chem.* 252:4449–4457.

Voglino, L., T. J. McIntosh, and S. A. Simon. 1998. Modulation of the binding of signal peptides to lipid bilayers by dipoles near the hydrocarbon-water interface. *Biochemistry.* 37:12241–12252.

Voglino, L., S. A. Simon, and T. J. McIntosh. 1999. Orientation of LamB signal peptides in bilayers: influence of lipid probes on peptide binding and interpretation of fluorescence quenching data. *Biochemistry.* 38: 7509–7516.

Wang, T.-Y., R. Leventis, and J. R. Silvius. 2000. Fluorescence-based evaluation of the partitioning of lipids and lipidated peptides into liquid-ordered lipid microdomains: a model for molecular partitioning into "lipid rafts." *Biophys. J.* 79:919–933.

Webb, R. J., J. M. East, R. P. Sharma, and A. G. Lee. 1998. Hydrophobic mismatch and the incorporation of peptides into lipid bilayers: a possible mechanism for retention in the Golgi. *Biochemistry.* 37:673–679.

Wieprecht, T., O. Apostolov, M. Beyermann, and J. Seelig. 2000. Interaction of a mitochondrial presequence with lipid membranes: role of helix formation for membrane binding and perturbation. *Biochemistry.* 39: 15297–15303.

Xu, X., and E. London. 2000. The effect of sterol structure on membrane lipid domains reveals how cholesterol can induce lipid domain formation. *Biochemistry.* 39:843–849.